

**You might find this additional information useful...**

---

This article cites 48 articles, 19 of which you can access free at:

<http://jn.physiology.org/cgi/content/full/94/2/1037#BIBL>

This article has been cited by 5 other HighWire hosted articles:

**Visualizing form and function in organotypic slices of the adult mouse parotid gland**

J. D. Warner, C. G. Peters, R. Saunders, J. H. Won, M. J. Betzenhauser, W. T. Gunning III, D. I. Yule and D. R. Giovannucci

*Am J Physiol Gastrointest Liver Physiol*, September 1, 2008; 295 (3): G629-G640.

[Abstract] [Full Text] [PDF]

**Increased secretory capacity of mouse adrenal chromaffin cells by chronic intermittent hypoxia: involvement of protein kinase C**

B. A. Kuri, S. A. Khan, S.-A. Chan, N. R. Prabhakar and C. B. Smith

*J. Physiol.*, October 1, 2007; 584 (1): 313-319.

[Abstract] [Full Text] [PDF]

**Dysregulation of brain-derived neurotrophic factor expression and neurosecretory function in *mecp2* null mice.**

H. Wang, S.-a. Chan, M. Ogier, D. Hellard, Q. Wang, C. Smith and D. M. Katz

*J. Neurosci.*, October 18, 2006; 26 (42): 10911-10915.

[Abstract] [Full Text] [PDF]

**Important Contribution of {alpha}-Neurexins to Ca<sup>2+</sup>-Triggered Exocytosis of Secretory Granules**

I. Dudanova, S. Sedej, M. Ahmad, H. Masius, V. Sargsyan, W. Zhang, D. Riedel, F.

Angenstein, D. Schild, M. Rupnik and M. Missler

*J. Neurosci.*, October 11, 2006; 26 (41): 10599-10613.

[Abstract] [Full Text] [PDF]

**CD24 is expressed by myofiber synaptic nuclei and regulates synaptic transmission**

M. Jevsek, A. Jaworski, L. Polo-Parada, N. Kim, J. Fan, L. T. Landmesser and S. J. Burden

*PNAS*, April 18, 2006; 103 (16): 6374-6379.

[Abstract] [Full Text] [PDF]

Updated information and services including high-resolution figures, can be found at:

<http://jn.physiology.org/cgi/content/full/94/2/1037>

Additional material and information about *Journal of Neurophysiology* can be found at:

<http://www.the-aps.org/publications/jn>

---

This information is current as of December 3, 2008 .

# Adrenal Chromaffin Cells Exhibit Impaired Granule Trafficking in NCAM Knockout Mice

Shyue-An Chan,<sup>1,\*</sup> Luis Polo-Parada,<sup>2,\*</sup> Lynn T. Landmesser,<sup>2</sup> and Corey Smith<sup>1,2</sup>

<sup>1</sup>Department of Physiology and Biophysics, <sup>2</sup>Department of Neurosciences, Case Western Reserve University, Cleveland, Ohio

Submitted 29 November 2004; accepted in final form 26 March 2005

**Chan, Shyue-An, Luis Polo-Parada, Lynn T. Landmesser, and Corey Smith.** Adrenal chromaffin cells exhibit impaired granule trafficking in NCAM knockout mice. *J Neurophysiol* 94: 1037–1047, 2005. First published March 30, 2005; doi:10.1152/jn.01213.2004. Neural cell adhesion molecule (NCAM) plays several critical roles in neuron path-finding and intercellular communication during development. In the clinical setting, serum NCAM levels are altered in both schizophrenic and autistic patients. NCAM knockout mice have been shown to exhibit deficits in neuronal functions including impaired hippocampal long term potentiation and motor coordination. Recent studies in NCAM null mice have indicated that synaptic vesicle trafficking and active zone targeting are impaired, resulting in periodic synaptic transmission failure under repetitive physiological stimulation. In this study, we tested whether NCAM plays a role in vesicle trafficking that is limited to the neuromuscular junction or whether it may also play a more general role in transmitter release from other cell systems. We tested catecholamine release from neuroendocrine chromaffin cells in the mouse adrenal tissue slice preparation. We utilize electrophysiological and electrochemical measures to assay granule recruitment and targeting in wild-type and NCAM  $-/-$  mice. Our data show that NCAM  $-/-$  mice exhibit deficits in normal granule trafficking between the readily releasable pool and the highly release-competent immediately releasable pool. This defect results in a decreased rate of granule fusion and thus catecholamine release under physiological stimulation. Our data indicate that NCAM plays a basic role in the transmitter release mechanism in neuroendocrine cells through mediation of granule recruitment and is not limited to the neuromuscular junction and central synapse active zones.

## INTRODUCTION

Neural cell adhesion molecule (NCAM) was originally identified as a neural integral membrane protein that facilitated cell-cell adhesion and axonal fasciculation (Rutishauser et al. 1978, 1983). NCAM is found in three major isoforms that are derived through alternative splicing of a single gene (Cunningham et al. 1987). NCAM 120, 140, and 180 all exhibit an IgG domain-containing extracellular portion that plays a role in cell-cell interactions. The 140- and 180-kDa isoforms also contain intracellular domains whose functions are less well understood but include  $\text{nf}\kappa\text{B}$ -binding, cytoskeletal binding and other signaling motifs (Crossin and Krushel 2000; Suter and Forscher 1998). Despite the role NCAM plays in developmental processes, mice in which the NCAM gene has been knocked out are viable and grow to maturity (Cremer et al. 1994).

NCAM is widely distributed throughout neuronal tissues, including neurons and glia of both the central and peripheral nervous systems (Seki and Arai 1993). It is also expressed in

neuroendocrine cells of pancreatic islets and neurohypophysis (Langley et al. 1989) as well as chromaffin cells of the adrenal medulla (Grant et al. 1992). NCAM knockout mice show deficits in normal formation of the islets of Langerhans (Esni et al. 1999) where it was suggested that lack of NCAM may affect cadherin-mediated adhesion, leading to abnormal cell sorting and aggregation during development. Cancerous neuroendocrine cells express an altered isoform-specific NCAM expression profile compared with noncancerous cells, indicating that posttranslational modification may affect tumor-genesis in this cell class (Lahr and Mayerhofer 1995). However, the functional role and thus effect of the NCAM knock-out in individual neuroendocrine cells has not been addressed.

Recent studies have demonstrated a functional role for NCAM in regulation and maintenance of transmitter release in neuronal tissues. NCAM knockout mice exhibit neuromuscular synaptic transmission deficits under physiological stimulation that lead to locomotor impairment (Polo-Parada et al. 2001). Transmission failure in these mice may be the result of an improper development of the synaptic vesicle trafficking process. This was demonstrated by the co-existence of two separate modes of synaptic vesicle cycling in the neuromuscular junction (NMJ) of adult NCAM  $-/-$  mice (Polo-Parada et al. 2001). One route is characterized by vesicle release that is not limited to the active zones but occurs throughout the nerve terminal. This release mechanism is mainly evoked by calcium influx through L-type  $\text{Ca}^{2+}$  channels. Exocytosis is then followed by an endocytic path that is sensitive to brefeldin-A (BFA), an agent that inhibits vesicular budding from the endoplasmic reticulum. This mechanism is classified as an immature trafficking process and is normally only observed during development in wild-type mice. The second trafficking mechanism is characterized by exocytosis that is preferentially evoked by calcium influx through P/Q-type channels and leads to endosomal trafficking that is insensitive to BFA. This P/Q-channel-dependent, BFA-insensitive vesicle exo-endocytosis cycle has been classified as a mature phenotype in that it is normally observed as the sole trafficking route in NMJs of the adult mouse (Polo-Parada et al. 2001). In addition, vesicle fusion in the normal adult NMJ is restricted to active zones at the nerve-muscle contact site (Polo-Parada et al. 2001). It is not yet understood how loss of NCAM affects synaptic maturation, vesicle cycling and targeting on the molecular level. However, some insight is offered by mice lacking only the NCAM 180 isoform, where synaptic transmission relies on the mature P/Q-type  $\text{Ca}^{2+}$  influx path, is not BFA sensitive, but does lack

\* S.-A. Chan and L. Polo-Parada contributed equally to this work.

Address for reprint requests and other correspondence: C. Smith, Dept. of Physiology and Biophysics, Case Western Reserve University, Cleveland, OH 44106-4970 (E-mail: Corey.Smith@Case.Edu).

The costs of publication of this article were defrayed in part by the payment of page charges. The article must therefore be hereby marked "advertisement" in accordance with 18 U.S.C. Section 1734 solely to indicate this fact.

the proper vesicle targeting to the active zones at the neuromuscular contact site. Like the total NCAM  $-/-$  mice, the NCAM 180  $-/-$  mice also exhibit locomotor deficits (Polo-Parada et al. 2004). Taken together these data point to improper targeting of vesicles to the active zone, and not the persistence of BFA-sensitive cycling or P/Q type-dependent  $Ca^{2+}$  influx, as the cause of the synaptic deficit in NCAM knockout mice.

Neuroendocrine cells lack the specialized synaptic structures found at the NMJ. Given this difference we wondered whether NCAM  $-/-$  mice would express any exocytic abnormalities. Neuroendocrine chromaffin cells release catecholamine through exocytosis from large dense-core granules that employ molecular fusion machinery very similar to that utilized in the neuromuscular junction with the exception that the large dense core secretory granules dock and fuse with the cell surface in the absence of a specialized active zone structure. We tested several parameters of catecholamine release from chromaffin cells in tissue slices prepared from NCAM  $+/+$  as well as NCAM  $-/-$  mice. Electrochemical and electrophysiological techniques were employed to determine granule recruitment to the releasable state, fusion competence, and sustained levels of release under repetitive physiological stimulation. We report here that chromaffin cells from NCAM  $-/-$  mice exhibit deficiencies in transmitter release that are analogous to those found in the neuromuscular junction. We expand on this finding and provide evidence that show the deficit is due to an impaired recruitment of granules from the readily releasable pool (RRP) to the final highly fusogenic immediately releasable pool (IRP). These data indicate an elemental role for NCAM in the granule/vesicle trafficking mechanism in diverse secretory cell types and thus is not limited to the specialized neuronal active zone.

## METHODS

### *Adrenal slice preparation.*

Adult NCAM  $-/-$  and wild-type C57/BL6 mice (4- to 8-wk-old, Jackson Laboratories, Bar Harbor ME) were used in this study. NCAM  $-/-$  mice were originally generated by Cremer et al. (1994) in a C57/BL6 background. NCAM  $-/-$  homozygotes were confirmed by PCR analysis. All anesthesia and euthanasia protocols were reviewed and approved by the institutional animal care and use committee (IACUC) of Case Western Reserve University, an accredited oversight body (federal animal welfare assurance No. A3145-01). Animals were deeply anesthetized by halothane (Sigma, St. Louis MO) inhalation and killed by decapitation. Adrenal glands were immediately removed and immersed in ice-cold, low-calcium bicarbonate-buffered saline (BBS) containing (in mM) 140 NaCl, 2 KCl<sub>2</sub>, 0.1 CaCl<sub>2</sub>, 5 MgCl<sub>2</sub>, 26 NaHCO<sub>3</sub>, and 10 glucose that was gassed with 95% O<sub>2</sub>-5% CO<sub>2</sub> (all chemical were acquired from Fisher Scientific, Cleveland, OH, unless otherwise noted). Osmolarity of the BBS was ~310 mOsm. Glands were trimmed of excess fat and embedded in 3% low gelling point agarose (Sigma) that was prepared before hand by melting agar in low calcium BBS at 110°C followed by equilibration to 35°C. The agarose was gelled on ice after tissue embedding. The agarose block was trimmed to ~3-mm cubes that contained a single gland each and glued to a tissue stand of a vibrotome (WPI, Sarasota, FL). The tissue stand was then placed in a slicing chamber filled with ice-cold, bubbled, low-Ca<sup>2+</sup> BBS. Adrenal glands were sectioned into 200- $\mu$ m-thick slices. The slices were collected and kept in the low calcium BBS first at 35°C for 30 min, then at 25°C until recording.

**IMMUNOHISTOCHEMICAL ANALYSIS** Animals were deeply anesthetized and fixed by transcardiac perfusion with 60 ml of 3.7% form-

aldehyde (Sigma) in phosphate-buffered saline (PBS). Adrenal glands were removed postfix, stored in 30% sucrose overnight at 4°C, embedded in OCT, cryosectioned at 14  $\mu$ m, and mounted on superfrost slides (Fisher Scientific). Slides were then washed twice in PBS and permeabilized with PBS +0.1% triton for 30 min. Sections were blocked with a solution of 4% BSA in PBS for 1 h and incubated with anti-NCAM antibody (R025b; a gift of Dr. Urs Rutishauser, Memorial Sloan-Kettering Cancer Center, New York) overnight at 4°C. Sections were washed five times each for 15 min with PBS and incubated with a FITC-conjugated secondary antibody (Zymed, San Francisco, CA) for 2 h at room temperature. Sections were then washed with PBS five times each for 15 min and mounted with anti-fade medium (Prolong, Molecular Probes, Eugene, OR). Fluorescence signals were visualized on an Olympus IX70 microscope at either  $\times 40$  or  $\times 100$  magnification. Image stacks were captured at pixel-width  $z$  resolution (square voxels) and deconvolved with a constrained-iterative algorithm built into SlideBook image processing software (v 4.0; Intelligent Imaging Innovations, Denver, CO).

**WESTERN BLOT ANALYSIS** Mice were anesthetized and killed, and the adrenal glands were quickly removed. The adrenal medulla was dissected out and homogenized in HEPES extraction buffer (in mM: 25 HEPES, 150 NaCl, 1 EDTA) containing 1% NP-40 and protease inhibitor mixture (Roche Diagnostics, Mannheim, Germany). The solubilized protein concentrations were determined (BCA method; Pierce, Rockford, IL) and adjusted to 2  $\mu$ g/ml. To remove sialic acid, the extract was incubated for 1 h at 37°C with 0.08 U/ml Neuraminidase type X (Calbiochem, San Diego, CA). SDS sample buffer containing dithiothreitol was added to each sample and the proteins separated by SDS-PAGE according to the Laemmli method on a 5 or 15% gel. The proteins were transferred onto polyvinylidene fluoride membranes preabsorbed with a solution of PBS and 4% milk. The membranes were then probed with primary antibodies in PBS and 4% milk overnight at 4°C. All antibodies were obtained from Transduction Labs (BD, San Diego, CA) except for actin (Sigma). The membranes were then washed in PBS, 0.1% Triton X-100 and HRP-conjugated secondary antibody for 2 h. The membranes were again washed five times, 15 min each in PBS. An enhanced chemiluminescence kit (Promega, Madison WI) was used to expose the blots onto film.

**ELECTROPHYSIOLOGICAL RECORDING** All experiments were performed 2–8 h after slice preparation. Tissue slices were constantly superfused with normal Ca<sup>2+</sup> BBS during recording (adapted from Barbara et al. 1998) containing (in mM): 140 NaCl, 2 KCl<sub>2</sub>, 3 CaCl<sub>2</sub>, 2 MgCl<sub>2</sub>, 26 NaHCO<sub>3</sub>, and 10 glucose and gassed with 95% O<sub>2</sub>-5% CO<sub>2</sub>. The osmolarity was ~310 mOsm. The recording chamber volume was ~1.5 ml and the buffer flow was set at 1 ml/min. Tissue slices were held in place by silver wires placed over the agar margin and visualized using an upright microscope (Olympus, Melville, NY) equipped with a  $\times 40$  water-immersion objective.

Patch pipettes were pulled from borosilicate glass (4–5 M $\Omega$ ). They were partially coated with molten dental wax and lightly polished by a microforge (Narashige, Tokyo, Japan). All recordings in this study were performed in the perforated-patch configuration. The perforated patch pipette solution contained (in mM): 135 CsGlutamate, 10 HEPES-H, 9.5 NaCl, 0.5 TEA-Cl, and 0.53 amphotericin B. pH was adjusted to 7.3 and osmolarity was 305 mOsm. Amphotericin B was prepared as a 100 $\times$  stock solution in DMSO (tissue culture-tested, Sigma) twice daily and diluted into internal pipette solution every 2 h. The internal solution was back-filled into patch pipettes without tip-dipping. No correction for liquid junction potential was made in this study. Cells were chosen for patching based on their appearance and physical orientation within the slice. Preference was given to cells that exhibited homogeneous cytosol (un-mottled) and an accessible clean surface. An orientation was considered preferable if it left access for the carbon fiber on the capillary pole. Cells were perforated to a series resistance of no more than 30 M $\Omega$  (mean = 19.9  $\pm$  0.56 M $\Omega$ ,

$n = 112$ ) and held at  $-80$  mV. Leak currents were not corrected. Voltage-clamp records were acquired through an EPC-9 voltage-clamp amplifier (HEKA Elektronik, Lambrecht, Germany) under control of Pulse software (v 8.53; HEKA Elektronik). Cell capacitance ( $C_m$ ) was estimated using a software lock-in module based on the Lindau-Neher technique (Gillis 1995) implemented as the Sine + D.C. mode. A 323-Hz, 25-mV peak amplitude sine wave was applied to the holding potential, and the reversal potential of the lock-in module was set to 0 mV. Membrane current was sampled at 20 kHz, and  $C_m$  was calculated at 323 Hz from the average value of 62 points/sine cycle. Nonsecretory capacitance signals were eliminated from dual-pulse recordings as described in the literature (Moser and Neher 1997; Voets et al. 1999). Only cells with less than  $-60$  pA leak current were analyzed for this study (leak current was  $-28.4 \pm 6.58$  pA; prestimulus cell capacitance =  $8.86 \pm 1.01$  pF,  $n = 112$  cells).

**PEPTIDE TRANSFECTION PROTOCOL** The PP-19 peptide was synthesized by Sigma Genosys (The Woodlands, TX) after a previously published sequence (Gad et al. 2000). Cells were transfected by using the Chariot protein transfection method (Active Motif, Carlsbad, CA). The transfection reaction was altered from the manufacturer's suggested protocol to increase efficiency in the adrenal slice preparation (Chan and Smith 2003). The reactions were prepared as follows: 2 ng Chariot reagent were dissolved in 50  $\mu$ l distilled water, the peptide was prepared as a solution of 500 ng protein in 50  $\mu$ l normal BBS. These solutions were mixed, sonicated, and kept at room temperature for 30 min to allow the Chariot-peptide complex to form. The Chariot/peptide complex mixture was then diluted to a final volume of 5 ml by low- $\text{Ca}^{2+}$  BBS, and bubbled with 95%  $\text{O}_2$ -5%  $\text{CO}_2$ . Maximum transfection efficiency was determined as the PP-19 concentration at which no further increase in PP-19 resulted in a greater difference in recorded behavior from control cells. Incomplete or sub-optimal transfection of cells with PP-19 would lead to an increased variance in measured granule exocytosis. However, this potential error would equally effect both NCAM  $+/+$  and  $-/-$  cells and thus would decrease the likelihood for detection of any knock out-dependent phenotype. Slices were incubated in this mixture for  $\geq 1$  h prior to recording.

**ELECTROCHEMICAL CATECHOLAMINE DETECTION** Commercially available carbon fiber electrodes (ALA Scientific, Longneck, NY) of 5- $\mu$ m tip diameter were used for amperometric catecholamine detection (Wightman et al. 1991). Carbon fibers were cut prior to each recording. A +650-mV potential was placed on the carbon fiber once it was in the bath, and the background current was allowed to relax to a steady value. If the resting current was  $>15$  pA or was unstable, the fiber was re-cut or replaced. Amperometric currents were recorded through a dedicated amplifier (VA-10, ALA Scientific). The head stages for the VA-10 and EPC-9 amplifiers shared a common Ag-AgCl bath ground. To minimize cross-talk between them, a 10  $\Omega$  resistor was placed into the ground wire of the VA-10 to separate the ground planes. During recordings the fiber was placed as close to the capillary pole of the patched cell as possible without physically distorting the cell. Oxidative amperometric currents, indicating catecholamine release, were passed through an analogue 1-kHz Bessel filter and sampled at 20 kHz simultaneous to the voltage-clamp current records in the Pulse software.

Voltage-clamped chromaffin cells were stimulated by trains of simulated action potential waveforms or by square pulse depolarization. Simulated action potentials were composed of a three-step ramp as follows [start potential (mV), end potential (mV), duration (ms)]:  $-80, 50, 2.5; 50, -90, 2.5; -90, -80, 2.5$ . This wave form evoked  $\text{Na}^+$  and  $\text{Ca}^{2+}$  currents statistically identical to native action potentials (Chan and Smith 2001). All experiments were carried out at  $24$ - $27^\circ\text{C}$ , and data analysis was performed with IGOR Pro software (WaveMetrics, Lake Oswego, OR). All data are presented as means  $\pm$  SE. Statistical analysis of data sets was determined by the student's

paired  $t$ -test. Asterisks in figures indicate a statistical difference ( $P < 0.02$ ) from control values.

## RESULTS

### *Adrenal NCAM expression is limited to the medulla*

We assayed expression of NCAM within the adrenal medulla by immuno-histochemistry. Tissue slices were cut from NCAM wild-type ( $+/+$ ) and knock out ( $-/-$ ) mice and stained with a pan-anti-NCAM antibody raised against the extracellular domain (R025b). After staining, slides were imaged under bright field illumination to identify the medulla (Fig. 1A). The adrenal medulla is made up largely by adrenal chromaffin cells with a few vascular endothelial cells and terminals from the innervating splanchnic nerve (Carmichael 1986). The NCAM  $+/+$  slice showed strong immuno-fluorescence signal in the medulla but little in the cortex. The right image pair was taken of slices prepared from NCAM  $-/-$  mice and, as expected, exhibit almost no signal. A higher-magnification image of the NCAM  $+/+$  slice indicates that the anti-NCAM stains the periphery of the chromaffin cells and is not due to signal from only the vascular endothelium or nerve terminals (Fig. 1B). Western blot analysis of isolated adrenal medulla was performed as described in METHODS. Equal amounts of protein from adrenal medullae harvested from NCAM  $+/+$  and  $-/-$  mice were loaded into adjacent lanes, separated on a 15% poly-acrylamide gel, transferred to membrane and probed with the same pan anti-NCAM antibody (R025B). As shown in Fig. 1C, all three isoforms of NCAM are present in the wild-type medulla, with the 140-kDa form expressed at the highest level. As expected, no NCAM immuno-fluorescence signals were detectable in the NCAM  $-/-$  medulla. Taken together these data indicate that NCAM is expressed in the adult adrenal medulla of wild-type mice and that the 140-kDa isoforms is the most prevalent.

### *Physiological stimulation of NCAM $-/-$ chromaffin cells elicits less catecholamine release*

We measured granule fusion with the capacitance technique and catecholamine release by electrochemical amperometry. Normally capacitance measurements would reflect the sum activity of exocytic membrane addition as well as endocytic membrane retrieval from the cell surface. To better quantify exocytosis only, we inhibited endocytosis by acute cell transfection with the clathrin-blocking peptide PP-19. PP-19 disrupts the association of synaptojanin and endophilin, a necessary step in clathrin-mediated endocytosis (Gad et al. 2000) and has successfully been applied in this preparation. We have previously shown that mouse chromaffin cells stimulated at 15 Hz in situ recycle granule membrane exclusively by clathrin-mediated endocytosis and that PP-19 blocks this process (Chan and Smith 2003). We confirmed this also to be true in NCAM  $-/-$  cells (Fig. 2Ai); the evoked capacitance response was significantly larger in the PP-19 transfected cells, whereas catecholamine release measured by amperometry was equivalent (data not shown).

NCAM  $-/-$  mice exhibit periodic neuromuscular transmission failures under physiological stimulation (Polo-Parada et al. 2001). To determine if NCAM  $-/-$  chromaffin cells share

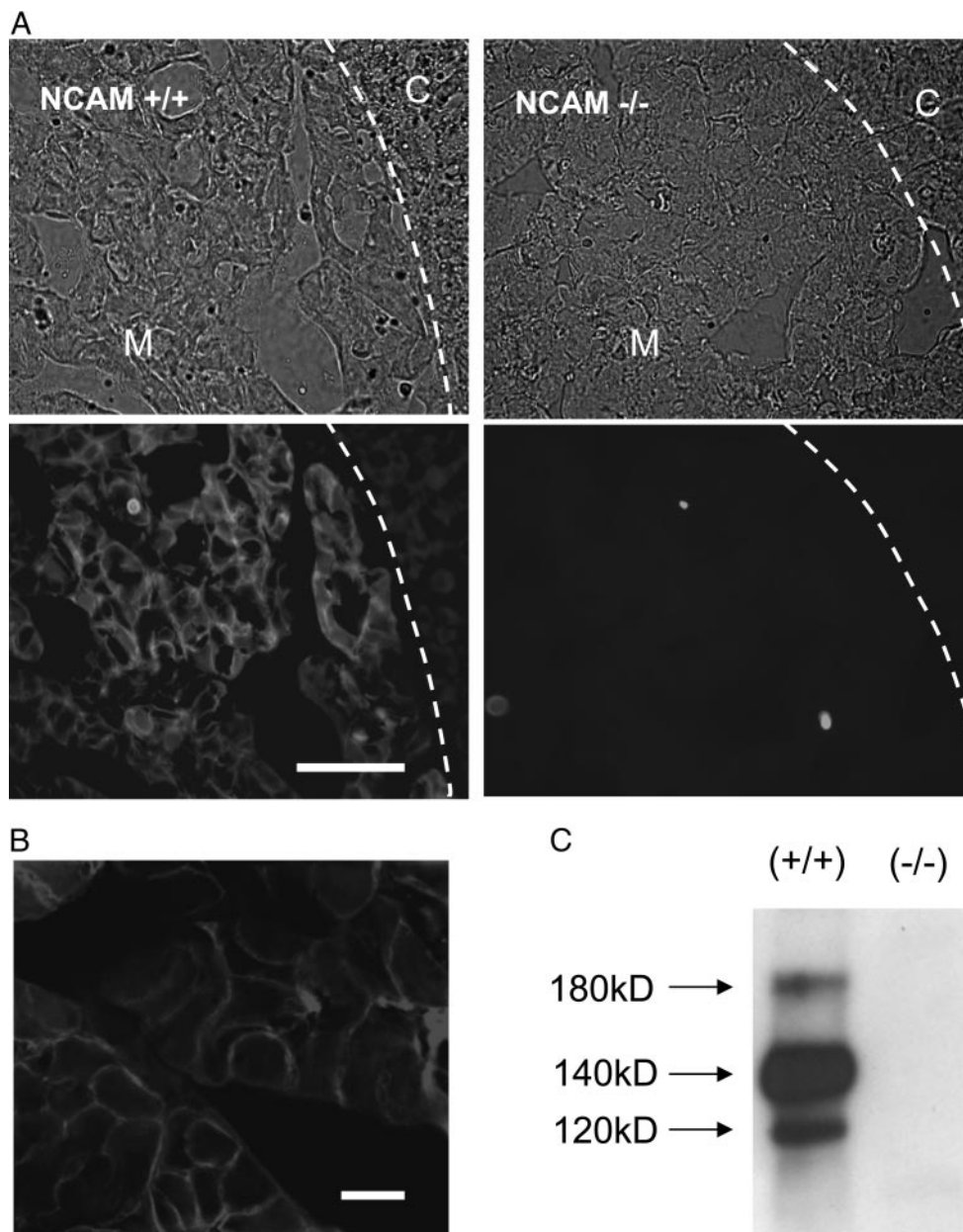


FIG. 1. Adrenal neural cell adhesion molecule (NCAM) expression is limited to the chromaffin cells of the medulla. *A*: Bright field (*top*) and NCAM immuno-fluorescence (*bottom*) are shown for NCAM +/+ (*left*) and -/- (*right*) tissues. NCAM was labeled with the pan-isoform antibody RO25b. ---, the adrenal medulla from the cortex. In NCAM +/+ mice, fluorescence signal is present in chromaffin cells (medulla; M), whereas no NCAM signal is detected in the adrenal cortex (C). Scale = 40  $\mu$ m. *B*: higher magnification reveals cell surface expression of NCAM in the wild-type mice. Scale bar = 10  $\mu$ m. *C*: Western blot analysis to determine NCAM isoform expression in the adrenal medulla. The blot demonstrates that all 3 isoforms of NCAM are present in NCAM +/+ mice, but none are expressed in the NCAM -/- mice.

this characteristic, we stimulated NCAM +/+ and -/- cells in situ at 15 Hz with action potential wave forms to mimic native sympathetic stimulation (Chan and Smith 2001). We measured evoked capacitance increases in PP-19 transfected cells to estimate granule fusion and carbon fiber amperometry to simultaneously measure catecholamine output.  $Ca^{2+}$  influx was measured as previously reported (Chan et al. 2003) as the peak  $Ca^{2+}$  current during the action potential depolarization. Records from NCAM +/+ and NCAM -/- cells ( $n = 9$  and 8, respectively) were averaged and are plotted in Fig. 2. The averaged capacitance traces (Fig. 2*Aii*) reveal that the NCAM -/- mice exhibit a deficit in evoked granule fusion. The

difference is not due to genotype-specific differences in evoked  $Ca^{2+}$  influx, which was equivalent in both cell types (*inset*). Representative amperometric records from single cells are provided in *Bi*. The average number of spikes per cell for each condition confirms that stimulation of NCAM -/- cells resulted in fewer exocytic events than in NCAM +/+ cells (*Bii*). We next estimated total catecholamine output by integrating capacitance signals (Fig. 2*C*). Total catecholamine release was significantly lower in NCAM -/- cells compared with +/+ cells ( $P < 0.02$ ). Thus as measured by membrane insertion, numbers of amperometric spikes and total catecholamine release, NCAM -/- cells show a secretory deficit under normal

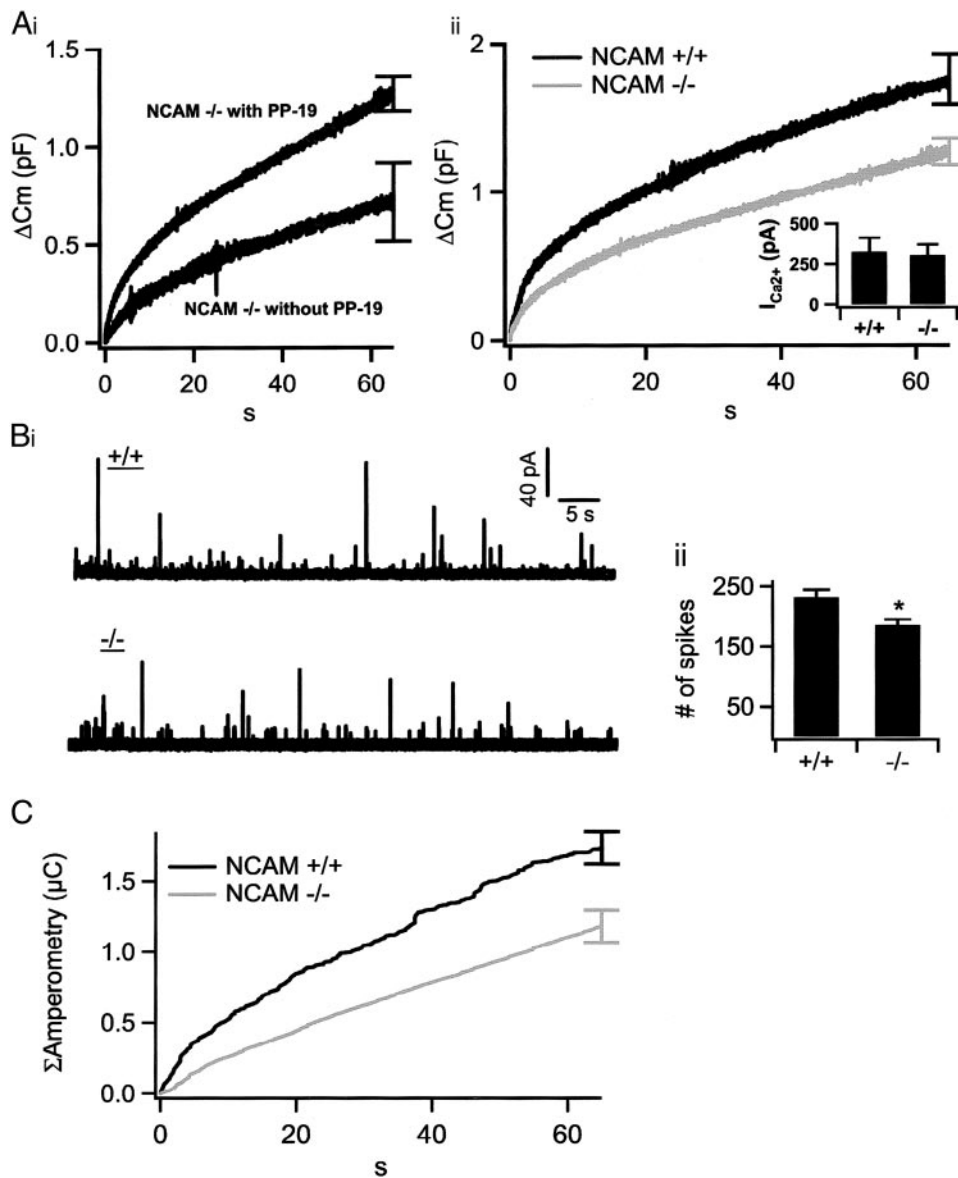


FIG. 2. NCAM  $-/-$  cells exhibit decreased exocytosis under physiological stimulation. *Ai*: PP-19 transfection blocks endocytosis in NCAM  $-/-$  chromaffin cells. Tissue slices cut from NCAM  $-/-$  mice were transfected with the PP-19 peptide (see METHODS for details) and stimulated with AP wave forms at 15 Hz. Data from this experiment are plotted together with data collected from untransfected cells ( $n = 6$  and  $8$ , respectively). The larger capacitance response in the PP-19-treated cells is due to a lack of endocytic membrane retrieval. Error bars at the end of each record represent the SE. *Aii*: wild-type and NCAM  $-/-$  chromaffin cells were stimulated at 15 Hz. Cells were transfected with the PP-19 peptide, thus capacitance reflects exocytosis alone. Cell capacitance records for each group were averaged ( $n = 9$  +/+;  $n = 8$  -/-) and plotted. Mean calcium currents evoked during each train were measured and averaged for all cells in both the NCAM +/+ and -/- cell-types (*inset*). *Bi*: catecholamine release was measured under each condition by carbon fiber amperometry. Representative recordings from NCAM +/+ and -/- cells are provided in *Bi*. *Bii*: this protocol was repeated on wild-type and NCAM knockout mice ( $n = 9$  and  $n = 8$ , respectively). Total numbers of spikes were counted for each condition and are plotted. *C*: total catecholamine release for each group was determined by integrating the entire amperometric records from *B*. The resulting average integrals are plotted. Error bars at the endpoint represent the SE of each data set.

physiological stimulation. Thus we set out to elucidate the underlying mechanism.

*Secretory deficit is due to a decreased number of granules in the IRP*

NCAM  $-/-$  mice exhibit a deficit in stimulus-evoked granule fusion and catecholamine release. We wondered what caused this secretory deficit. In Fig. 2, we showed that evoked  $Ca^{2+}$  influx in both NCAM +/+ and -/- mice is equivalent and therefore not the cause (Fig. 2*Aii*, *inset*). Two other potential sources for the phenotype were considered: the NCAM  $-/-$  cells exhibit a deficit in the “readily releasable” granule population that defines and limits stimulus-dependent secretion (Heinemann et al. 1993) or the NCAM  $-/-$  mice express an exocytic machinery with impaired  $Ca^{2+}$  sensing, thus causing a less steep stimulus-secretion function. We tested both possibilities.

The recruitment and maturation of chromaffin secretory granules to the fusion competent state has been well studied in bovine and mouse chromaffin and clonal PC-12 cells (Hay et

al. 1995; Heinemann et al. 1993; Parsons et al. 1995; Steyer et al. 1997). A prevailing mechanism describes a series of sequential recruitment steps from a large reserve granule pool to a RRP. From the RRP granules can either revert to the reserve pool, undergo exocytosis or enter a more fusogenic IRP through which granules fuse approximately fivefold faster than through the RRP (Voets et al. 1999). Action potential stimulation provides a very modest and brief  $Ca^{2+}$  signal, thus granules from the IRP can be expected to dominate the release process under physiological stimulation. We utilized a paired-pulse depression protocol to quantify the size of RRP and IRP in both wild-type and NCAM  $-/-$  mice. The RRP paired-pulse depression protocol was based on a previous study in isolated chromaffin cells (Gillis et al. 1996) and has been used extensively to quantify the number of granules resident at defined steps along the secretion path (Smith 1999; Smith et al. 1998; Voets et al. 1999; Yang et al. 2002). The dual-pulse protocol separates  $Ca^{2+}$  influx from the secretion process in that  $Ca^{2+}$  influx is sufficiently large that it is not the limiting

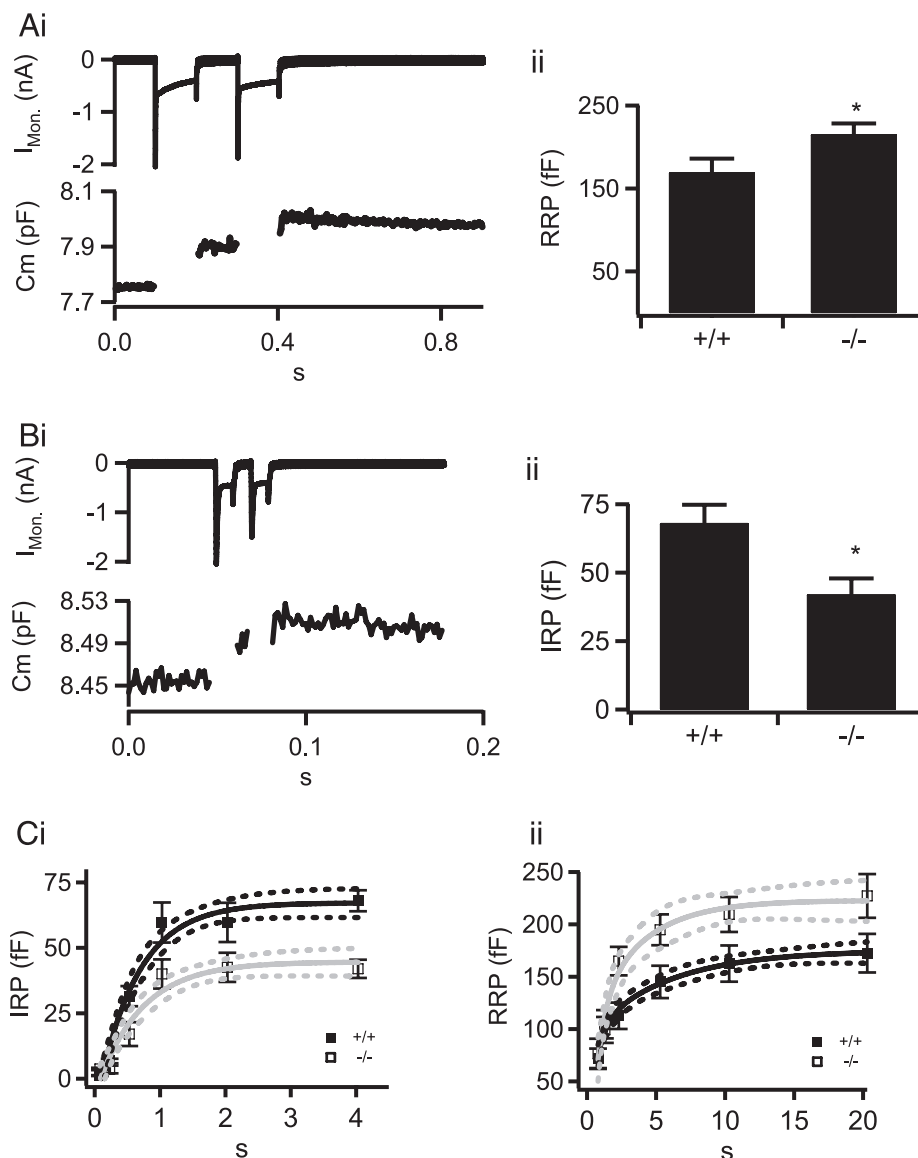


FIG. 3. The releasable granule pools are altered in NCAM  $-/-$  mice. Readily and immediately releasable granule pools (RRP and IRP, respectively) were quantified in both NCAM  $+/+$  and  $-/-$  chromaffin cells. *Ai*: the RRP was quantified as described (Gillis et al. 1996). Briefly cells were voltage clamped at  $-80$  mV and stimulated with a pair of 100-ms depolarizations first to 0 mV and then to  $+5$  mV to balance  $Ca^{2+}$  influx. *Top*: the evoked current influx. In the example recording provided, the first pulse resulted in a greater  $C_m$  increase than the second pulse ( $C_{m1}$  and  $C_{m2}$ , respectively). This is broadly interpreted as a consumption of release-ready granules by the first response leaving few for the second pulse to access. Formally, the RRP can thus be quantified as  $RRP = S/(1 - R^2)$  where  $S$  is the sum of  $C_{m1}$  and  $C_{m2}$  and  $R$  is the ratio of  $C_{m2}$  to  $C_{m1}$ . *Aii*: this dual-pulse RRP protocol was repeated on NCAM  $+/+$  and  $-/-$  cells. Only cells that exhibit strong depression ( $C_{m2}$  is small compared with  $C_{m1}$ ) provide an accurate estimate of the releasable pool size by the dual pulse method. For this reason, only cells that exhibited a depression ratio ( $C_{m2}/C_{m1}$ ) of  $\leq 0.7$  were included for further analysis. The quantified RRP sizes from NCAM  $+/+$  and NCAM  $-/-$  records ( $n = 36$  and  $32$ , respectively) are summarized and show that the RRP was significantly larger in the NCAM  $-/-$  cells. *Bi*: the IRP was measured as previously described (Voets et al. 1999) in NCAM  $+/+$  and  $-/-$  mice. This pool was measured as the paired-pulse depression in response to 10-ms stimuli to  $+5$  mV. As in *A*, data from a representative experiment are pictured. *Bii*: this protocol was repeated on NCAM  $+/+$  and  $-/-$  cells with those that exhibited a depression ratio of  $\geq 0.7$  chosen for further analysis ( $n = 22$  and  $23$ , respectively). The IRP was found to be significantly smaller in NCAM  $-/-$  cells. *C*: kinetic analysis of IRP (*i*) and RRP (*ii*) refilling. For each cell type, the IRP ( $+/+ n = 25$ ,  $-/- n = 23$ ) or RRP ( $+/+ n = 21$ ,  $-/- n = 27$ ) was depleted by delivering a dual-pulse protocol as in *A* and *B*. A 2nd pulse-pair was then delivered at various times after initial depletion to probe the degree of refilling in a time-dependent manner. Because the IRP is considered a subset of the RRP, we first fit the IRP refilling curves with a mono-exponential function (—, the best fit; ---, 1/e confidence bands, *Ci*) and then used the measured refilling rate constant as a fixed term in a double exponential fit for the RRP refilling curves (—, the best fit; ---, 1/e confidence bands, *Cii*). The 2nd slower exponential thus represents the refilling of the RRP alone.

factor for secretion, rather the number of granules defines the magnitude of the response. Briefly, two 100-ms square pulse stimuli were delivered at a 100-ms interval and their amplitudes were adjusted to evoke equivalent amounts of  $Ca^{2+}$  entry (Fig. 3*Ai*). The first  $Ca^{2+}$  influx causes secretion and depletion of the RRP, leaving fewer granules for release during to the

second  $Ca^{2+}$  influx. This results in a depletion-dependent secretory depression in response to the second pulse. The evoked capacitance response for each pulse was measured and their magnitudes used to calculate the total number of release-ready granules (see Fig. 3 legend) (see also Gillis et al. 1996 for a full description of the technique). The results from this



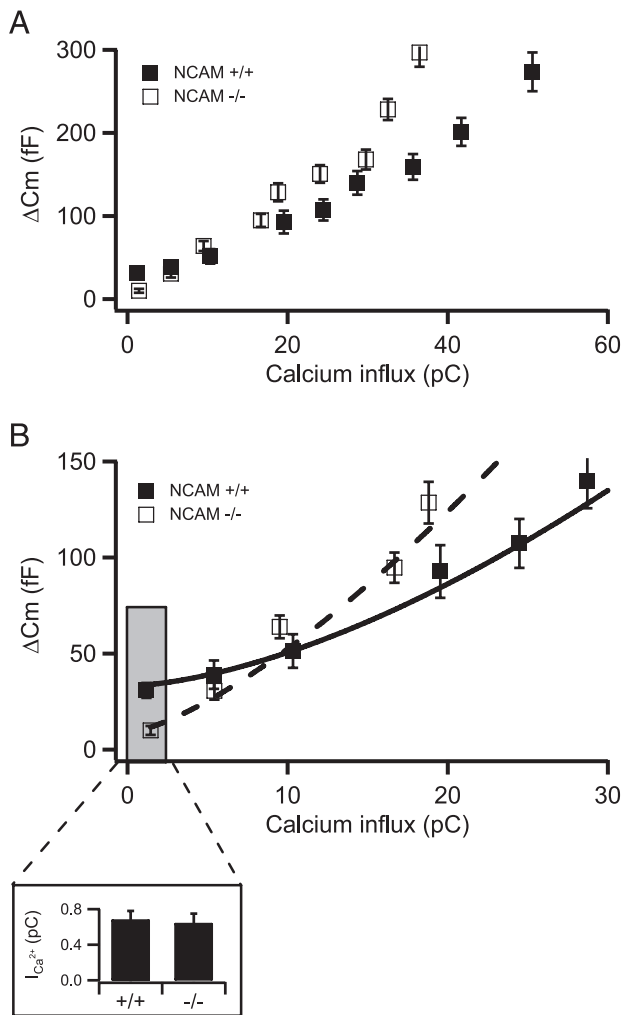


FIG. 4. A granule recruitment deficit is responsible for the lessened exocytosis under physiological stimulation. *A*: cells were stimulated to quantify secretion as a function of stimulus strength. In this protocol, cells were stimulated with randomized, variable duration square pulse depolarizations to +5 mV. Cell capacitance values are plotted against integrated  $Ca^{2+}$  influx, utilized as an index of stimulus strength. At lower stimulus amplitudes, the NCAM  $-/-$  cells exhibited a weaker stimulus-secretion coupling, but stronger coupling with increased stimulation. *B*: the lower stimulus range of the plot in *A* is shown to better examine the secretory behavior under  $Ca^{2+}$  influx levels expected during physiological stimulation ( $\square$ ). *Inset*: mean  $Ca^{2+}$  influx evoked per action potential during 15-Hz stimulation in NCAM  $-/-$  and  $+/+$  mice. Despite the overall steeper stimulus-secretion function found in the NCAM  $-/-$  mice, the expected release at levels matching physiological stimulation is smaller in the knock-outs.

#### PMA and ML-9 invert NCAM $-/-$ and $+/+$ phenotypes

We previously showed that treatment of NCAM  $-/-$  NMJs with the phorbol ester phorbol-12-myristate-13-acetate (PMA) rescues transmission failures normally observed under repetitive stimulation (Polo-Parada et al. 2001, 2004). We also demonstrated that granule recruitment and secretion is regulated by a PMA-sensitive process in isolated bovine chromaffin cells through activation of protein kinase C (PKC) (Smith 1999; Smith et al. 1998). Last, we found that block of myosin light chain kinase with the agent ML-9 induces synaptic failures in NMJs of NCAM  $+/+$  mice, mimicking the phenotype of NCAM  $-/-$  mice. Work by others has shown a link between MLCK and granule availability in chromaffin cells

(Gasman et al. 1998; Li et al. 2003). We asked if PMA and ML-9 would produce effects in mouse chromaffin cells under physiological stimulation similar to those observed in the NMJ. We blocked clathrin-mediated endocytosis as previously described (Chan and Smith 2003) to isolate exocytosis in the capacitance recording (see also Fig. 2). We then pretreated NCAM  $-/-$  and NCAM  $+/+$  tissue slices for 5 min with 100 nM PMA or 15  $\mu$ M ML-9, respectively, and stimulated the cells at 15 Hz. The results from these experiments are presented in Fig. 6 and show that, as in the NMJ, phorbol ester treatment of the NCAM  $-/-$  cells completely rescues the secretory deficit seen in untreated cells. Furthermore, the static IRP measured from PMA-treated NCAM  $-/-$  cells was identical to that measured in untreated NCAM  $+/+$  cells ( $66.3 \pm 7.96$  and  $68.96 \pm 7.05$  fF, respectively). Conversely, pretreatment of NCAM  $+/+$  cells with ML-9 decreased secretory output to a level similar to that observed in untreated NCAM  $-/-$  cells (Fig. 6). Last, as a control we treated NCAM  $-/-$  cells with ML-9, which would be predicted to have no effect. Indeed this was the case, no change in secretion was measured between untreated and ML-9-treated NCAM  $-/-$  cells.

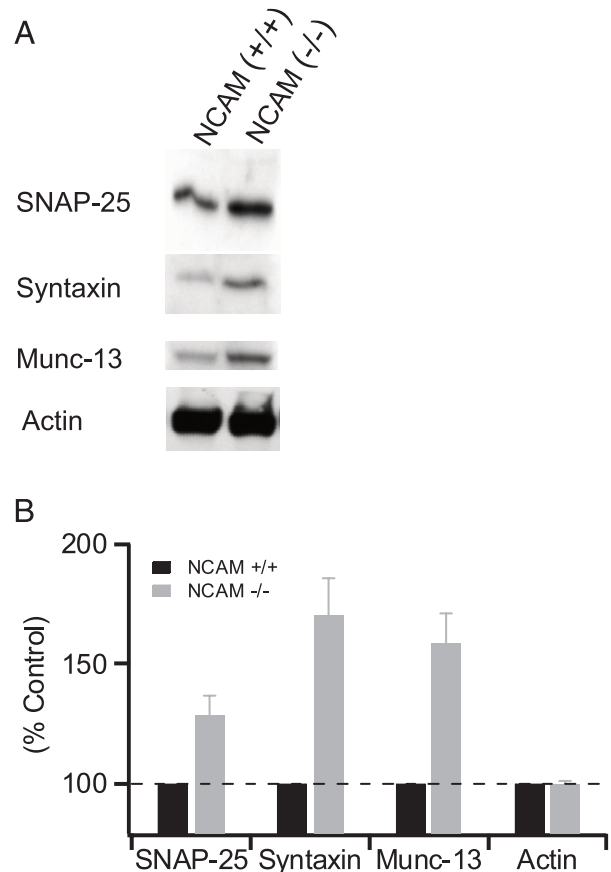


FIG. 5. SNARE complex proteins are overexpressed in NCAM  $-/-$  mice. *A*: a potential compensation mechanism for the granule trafficking deficit may explain the steeper stimulus-secretion function found in NCAM  $-/-$  mice. Western blot analysis was performed on equal amounts of protein collected from NCAM  $-/-$  and  $+/+$  adrenal medullary tissues. Proteins were separated by PAGE electrophoresis and probed with antibodies to SNAP-25, Syntaxin, and Munc-13, all key SNARE complex proteins. Actin levels serve as a loading control. *B*: densitometry was performed on the blots to quantify expression of each protein in the NCAM  $-/-$  adrenal medullae.

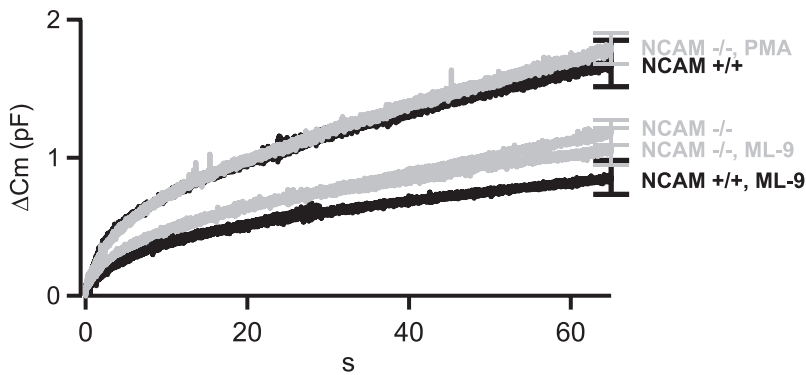


FIG. 6. PKC rescues the NCAM  $-/-$  phenotype and ML-9 mimics the knockout phenotype. The protocol presented in Fig. 2 was repeated on NCAM  $-/-$  tissue slices pretreated with either 100 nM PMA or NCAM  $+/+$  slices pretreated with 15  $\mu$ M ML-9 for 5 min ( $n = 11$  and  $22$ , respectively). PMA treatment of NCAM  $-/-$  cells resulted in secretion levels nearly identical to wild-type, whereas ML-9 treatment of NCAM  $+/+$  cells decreased evoked capacitance signals to below those observed in the NCAM  $-/-$  cells. We also treated NCAM  $-/-$  cells with ML-9 and found no effect ( $n = 6$ ). Data for untreated cells are re-plotted from Fig. 2 for comparison. Error bars are shown for the final point in each record and represent the SE.

## DISCUSSION

A rich literature describes a critical role for NCAM in axon guidance and stabilization of central synapses during development. However, more recently NCAM has been shown to retain an important role after development, it has been shown to be important in aspects of synaptic stabilization and function in the adult animal (Cremer et al. 1998; Muller et al. 1996; Polo-Parada et al. 2001, 2004; Rafuse et al. 2000). Data from these studies combine to demonstrate that NCAM  $-/-$  mice exhibit deficits in both central hippocampal and cerebellar synaptic plasticity as well as peripheral neuromuscular synaptic transmission. The synaptic systems in all these studies signal through the fusion of vesicles at specialized presynaptic active zones. This shared characteristic lead to the suggestion that NCAM may play a structural role in active zone stabilization, somewhat similar to the intercellular adhesion function served during development (Moscoso et al. 1998; Rutishauser and Landmesser 1991, 1996). However, the data collected from the neuroendocrine chromaffin cells point to a more basic function for NCAM in that this cell type does not release granules at a structurally identifiable active zone. This opens the possibility that NCAM may be an important molecule in the regulation and proper function of secretory cells in general and is not restricted to specialized active zones found in neurons. In the current study, we present data demonstrating that evoked catecholamine release is decreased in NCAM knock out mice. In addition, we demonstrate that the secretory deficit in NCAM  $-/-$  mice is due to a slower transfer of granules from the RRP into the IRP. Granule fusion and transmitter release can occur either from the RRP or the IRP. However, the rate constant for granule fusion from the IRP is  $\geq 5$ -fold faster than that from the RRP (Voets et al. 1999) and is expected to represent the vast majority of catecholamine release under mild stimulation. Thus the smaller IRP found in the NCAM  $-/-$  mice would directly decrease the rate of granule exocytosis under physiological stimulation in which  $Ca^{2+}$  influx is modest.

Such functional abnormalities would be predicted to result in detrimental misregulation of many organ and homeostatic systems that fall under the control of the sympathetic nervous system and catecholamine release. We hypothesized that lowered catecholamine levels would lead to a lower vascular tone and thus decreased mean arterial pressure in the knockout mice. Indeed, we did measure lower blood pressure in the NCAM  $-/-$  versus  $+/+$  mice, but it failed to reach significance. This could be partially attributed to alteration of other secretory systems (i.e., increased renin secretion from the

kidney). The lack of pathophysiology that are expected from disruption of neuroendocrine output points to a compensation for the secretory deficit. This may reside at the cellular level. We found that the NCAM  $-/-$  mice overexpress proteins vital to the secretory process (SNAP-25, Syntaxin, and Munc-13). Such an overexpression is consistent with a compensation mechanism designed to facilitate more complete fusion of the granules within the remaining IRP or to enhance the rate of fusion from the RRP. This would be achieved by increasing the copy number of fusion machines per granule. However, this overexpression is insufficient to rescue the NCAM-dependent trafficking deficit responsible for impaired catecholamine release. Additional potential compensatory sites could include the upregulation of end-organ adrenergic receptor expression and/or downregulation of the corresponding parasympathetic nervous system activity. Possible compensation for NCAM-dependent neuroendocrine abnormalities have been described in other secretory systems. Organization and polarity of insulin-secreting pancreatic  $\beta$ -cells is altered in NCAM knock out mice and is similar to that found in humans suffering from type-II diabetes mellitus (Esní et al. 1999). However, Esní and colleagues found glucose levels in these mice to be normal.

Potential systems-level compensatory mechanisms notwithstanding, on the cellular level NCAM  $-/-$  chromaffin cells exhibit a secretory phenotype that is due to a decreased retention of granules in the IRP. This, combined with the quantitative experimental and analytic techniques available in chromaffin cells, will allow further definition of the regulatory role played by NCAM in the exocytic process. Previous studies in the neuromuscular junction have shown that the NCAM-dependent secretory deficit can be overcome by treating the cells with phorbol esters such as PMA (Polo-Parada et al. 2001). Here we confirm this finding to be true in chromaffin cells (Fig. 6); indeed PMA treatment restores the IRP in NCAM  $-/-$  mice to control values. PMA increases stimulus-dependent exocytosis in chromaffin cells (Gillis et al. 1996) as well as in other neuronal preparations (Stevens and Sullivan 1998) by facilitating the recruitment of granules to the readily releasable pool through activation of protein kinase C. Indeed, prolonged stimulation of chromaffin cells with depolarizing trains results in a persistent secretory facilitation through  $Ca^{2+}$ -dependent activation of PKC (Smith 1999). Further experiments will determine the exact nature and orientation of NCAM and PKC in the secretory granule recruitment process.

Other trafficking mechanisms may involve an NCAM-associated vesicle mobilization step. For example, it is known that in chromaffin cells (Matsumura et al. 1999; Neco et al. 2002),

hippocampal cultured neurons (Ryan 1999), and superior cervical ganglion cells (Mochida 1995), vesicle mobilization is dependent on the normal function of myosin light-chain kinase (MLCK). Similar results were obtained in the neuromuscular junction where block of MLCK mimics the synaptic transmission failures observed in NCAM  $-/-$  mice (Polo-Parada et al. 2001, 2004). This finding was also repeated in the current study where ML-9 treatment of NCAM  $+/+$  cells depresses granule fusion to a level observed in untreated NCAM  $-/-$  cells. The function of MLCK in catecholamine exocytosis would be part of a more complex signaling path; it has been shown recently that specific NCAM isoforms interact with components of the cytoskeleton including  $\alpha$ - and  $\beta$ -tubulin,  $\alpha$ - and  $\beta$ -actin, tropomyosin, microtubulin-associated protein (MAP 1A) and rho kinase (Buttner et al. 2003). Rho-kinases play a role in the modulation of MLCK activity and have recently been shown to regulate activity-dependent mobilization and fusion of chromaffin granules (Gasman et al. 1998; Li et al. 2003). Together these results point to a potential association of NCAM- and MLCK-dependent processes in the recruitment of secretory organelles in general. These elements may provide a molecular complex allowing proper granule trafficking in normal cells and may explain the deficit in the IRP in the NCAM  $-/-$  mice. Ongoing and future experiments in chromaffin cells will clarify the NCAM-dependent mechanism in the evoked release of signaling molecules.

#### ACKNOWLEDGMENTS

We are grateful to Dr. Ur Rutishauser (Memorial Sloan-Kettering Cancer Center) for the gift of the R025b pan anti-NCAM antibody. We thank G. Pilar and K. Trueblood for critical comments during preparation of the manuscript.

#### GRANTS

This work was supported by a grant from the National Science Foundation to C. Smith (IBN-0196136), American Heart Association Grant 0530140N to L. Polo-Parada, and National Institute of Neurological Disorders and Stroke Grants NS-19640 and NS-23678 to L. T. Landmesser.

#### REFERENCES

- Barbara JG, Lemos VS, and Takeda K. Pre- and post-synaptic muscarinic receptors in thin slices of rat adrenal gland. *Eur J Neurosci* 10: 3535–3545, 1998.
- Burgoyne RD and Morgan A. Analysis of regulated exocytosis in adrenal chromaffin cells: insights into NSF/SNAP/SNARE function. *Bioessays* 20: 328–335, 1998.
- Burgoyne RD, Morgan A, Barnard RJ, Chamberlain LH, Glenn DE, and Kibble AV. SNAPs and SNAREs in exocytosis in chromaffin cells. *Biochem Soc Trans* 24: 653–657, 1996.
- Buttner B, Kannicht C, Reutter W, and Horstkorte R. The neural cell adhesion molecule is associated with major components of the cytoskeleton. *Biochem Biophys Res Commun* 310: 967–971, 2003.
- Carmichael SW. Morphology and innervation of the adrenal medulla. In: *Stimulus-Secretion Coupling*, edited by Rosenheck K and Lelkes P. Boca Raton, FL: CRC, 1986, vol. 1, p. 40–49.
- Chan SA, Chow R, and Smith C. Calcium dependence of action potential-induced endocytosis in chromaffin cells. *Pfluegers* 445: 540–546, 2003.
- Chan SA and Smith C. Physiological stimuli evoke two forms of endocytosis in bovine chromaffin cells. *J Physiology* 537: 871–885, 2001.
- Chan SA and Smith C. Low frequency stimulation of mouse adrenal slices reveals a clathrin-independent, protein kinase C-mediated endocytic mechanism. *J Physiol* 553.3: 707–717, 2003.
- Cremer H, Chazal G, Carleton A, Goridis C, Vincent JD, and Lledo PM. Long-term but not short-term plasticity at mossy fiber synapses is impaired in neural cell adhesion molecule-deficient mice. *Proc Natl Acad Sci USA* 95: 13242–13247, 1998.
- Cremer H, Lange R, Christoph A, Plomann M, Vopper G, Roes J, Brown R, Baldwin S, Kraemer P, Scheff S, Borthois D, Rajewsky K, and Wille W. Inactivation of the N-CAM gene in mice results in size reduction of the olfactory bulb and deficits in spatial learning. *Nature* 367: 455–459, 1994.
- Crossin KL and Krushel LA. Cellular signaling by neural cell adhesion molecules of the immunoglobulin superfamily. *Dev Dyn* 218: 260–279, 2000.
- Cunningham BA, Hemperly JJ, Murray BA, Prediger EA, Brackenbury R, and Edelman GM. Neural cell adhesion molecule: structure, immunoglobulin-like domains, cell surface modulation, and alternative RNA splicing. *Science* 236: 799–806, 1987.
- Engisch KL, Chervenetskaya NI, and Nowycky MC. Short-term changes in the  $Ca^{2+}$ -exocytosis relationship during repetitive pulse protocols in bovine adrenal chromaffin cells. *J Neurosci* 17: 9010–9025, 1997.
- Engisch KL and Nowycky MC. Calcium dependence of large dense-cored vesicle exocytosis evoked by calcium influx in bovine adrenal chromaffin cells. *J Neurosci* 16: 1359–1369, 1996.
- Esni F, Taljedal IB, Perl AK, Cremer H, Christofori G, and Semb H. Neural cell adhesion molecule (N-CAM) is required for cell type segregation and normal ultrastructure in pancreatic islets. *J Cell Biol* 144: 325–337, 1999.
- Gad H, Ringstad N, Low P, Kjaerulff O, Gustafsson J, Wenk M, Di Paolo G, Nemoto Y, Crun J, Ellisman MH, De Camilli P, Shupliakov O, and Brodin L. Fission and uncoating of synaptic clathrin-coated vesicles are perturbed by disruption of interactions with the SH3 domain of endophilin. *Neuron* 27: 301–312, 2000.
- Gasman S, Chasserot-Golaz S, Hubert P, Aunis D, and Bader MF. Identification of a potential effector pathway for the trimeric Go protein associated with secretory granules. Go stimulates a granule-bound phosphatidylinositol 4-kinase by activating RhoA in chromaffin cells. *J Biol Chem* 273: 16913–16920, 1998.
- Gillis KD. Techniques for membrane capacitance measurements. In: *Single-Channel Recording, Second Edition*, edited by Sakmann B and Neher E. New York: Plenum, 1995, chapt. 7, p. 155–198.
- Gillis KD, Mossner R, and Neher E. Protein kinase C enhances exocytosis from chromaffin cells by increasing the size of the readily releasable pool of secretory granules. *Neuron* 16: 1209–1220, 1996.
- Graham ME, Washbourne P, Wilson MC, and Burgoyne RD. Molecular analysis of SNAP-25 function in exocytosis. *Ann NY Acad Sci* 971: 210–221, 2002.
- Grant NJ, Leon C, Aunis D, and Langley K. Cellular localization of the neural cell adhesion molecule L1 in adult rat neuroendocrine and endocrine tissues: comparisons with NCAM. *J Comp Neurol* 325: 548–558, 1992.
- Hay JC, Fiset PL, Jenkins GH, Fukami K, Takenawa T, Anderson RA, and Martin TF. ATP-dependent inositol phosphorylation required for  $Ca^{2+}$ -activated secretion. *Nature* 374: 173–177, 1995.
- Heinemann C, von Ruden L, Chow RH, and Neher E. A two-step model of secretion control in neuroendocrine cells. *Pfluegers Arc Eur J Physiol* 424: 105–112, 1993.
- Lahr G and Mayerhofer A. Expression of the neural cell adhesion molecule NCAM by peptide- and steroid-producing endocrine cells and tumors: alternatively spliced forms and polysialylation. *Endocr Pathol* 6: 91–101, 1995.
- Langley O, Aletsee UM, Grant N, and Gratzl M. Expression of the neural cell adhesion molecule NCAM in endocrine cells. *J Histochem Cytochem* 37: 781–791, 1989.
- Li Q, Ho CS, Marinescu V, Bhatti H, Bokoch GM, Ernst SA, Holz RW, and Stuenkel EL. Facilitation of  $Ca^{2+}$ -dependent exocytosis by Rac1-GTPase in bovine chromaffin cells. *J Physiol* 550: 431–445, 2003.
- Matsumura C, Kuwashima H, and Kimura T. Myosin light chain kinase inhibitors and calmodulin antagonist inhibit  $Ca^{2+}$ - and ATP-dependent catecholamine secretion from bovine adrenal chromaffin cells. *J Auton Pharmacol* 19: 115–121, 1999.
- Mochida S. Role of myosin in neurotransmitter release: functional studies at synapses formed in culture. *J Physiol* 89: 83–94, 1995.
- Moscoco LM, Cremer H, and Sanes JR. Organization and reorganization of neuromuscular junctions in mice lacking neural cell adhesion molecule, tenascin-C, or fibroblast growth factor-5. *J Neurosci* 18: 1465–1477, 1998.
- Moser T and Neher E. Rapid exocytosis in single chromaffin cells recorded from mouse adrenal slices. *J Neurosci* 17: 2314–2323, 1997.
- Muller D, Wang C, Skibo G, Toni N, Cremer H, Calaora V, Rougon G, and Kiss JZ. PSA-NCAM is required for activity-induced synaptic plasticity. *Neuron* 17: 413–422, 1996.
- Neco P, Gil A, Del Mar Frances M, Viniestra S, and Gutierrez LM. The role of myosin in vesicle transport during bovine chromaffin cell secretion. *Biochem J* 368: 405–413, 2002.

- Parsons TD, Coorsen JR, Horstmann H, and Almers W.** Docked granules, the exocytic burst, and the need for ATP hydrolysis in endocrine cells. *Neuron* 15: 1085–1096, 1995.
- Polo-Parada L, Bose CM, and Landmesser LT.** Alterations in transmission, vesicle dynamics, and transmitter release machinery at NCAM-deficient neuromuscular junctions. *Neuron* 32: 815–828, 2001.
- Polo-Parada L, Bose CM, Plattner F, and Landmesser LT.** Distinct roles of different neural cell adhesion molecule (NCAM) isoforms in synaptic maturation revealed by analysis of NCAM 180 kDa isoform-deficient mice. *J Neurosci* 24: 1852–1864, 2004.
- Rafuse VF, Polo-Parada L, and Landmesser LT.** Structural and functional alterations of neuromuscular junctions in NCAM-deficient mice. *J Neurosci* 20: 6529–6539, 2000.
- Rutishauser U, Gall WE, and Edelman GM.** Adhesion among neural cells of the chick embryo. IV. Role of the cell surface molecule CAM in the formation of neurite bundles in cultures of spinal ganglia. *J Cell Biol* 79: 382–393, 1978.
- Rutishauser U, Grumet M, and Edelman GM.** Neural cell adhesion molecule mediates initial interactions between spinal cord neurons and muscle cells in culture. *J Cell Biol* 97: 145–152, 1983.
- Rutishauser U and Landmesser L.** Polysialic acid in the vertebrate nervous system: a promoter of plasticity in cell-cell interactions. *Trends Neurosci* 19: 422–427, 1996.
- Rutishauser U and Landmesser L.** Polysialic acid on the surface of axons regulates patterns of normal and activity-dependent innervation. *Trends Neurosci* 14: 528–532, 1991.
- Ryan TA.** Inhibitors of myosin light chain kinase block synaptic vesicle pool mobilization during action potential firing. *J Neurosci* 19: 1317–1323, 1999.
- Seki T and Arai Y.** Distribution and possible roles of the highly polysialylated neural cell adhesion molecule (NCAM-H) in the developing and adult central nervous system. *Neurosci Res* 17: 265–290, 1993.
- Smith C.** A persistent activity-dependent facilitation in chromaffin cells is caused by  $\text{Ca}^{2+}$  activation of protein kinase C. *J Neurosci* 19: 589–598, 1999.
- Smith C, Moser T, Xu T, and Neher E.** Cytosolic  $\text{Ca}^{2+}$  acts by two separate pathways to modulate the supply of release-competent vesicles in chromaffin cells. *Neuron* 20: 1243–1253, 1998.
- Stevens CF and Sullivan JM.** Regulation of the readily releasable vesicle pool by protein kinase C. *Neuron* 21: 885–893, 1998.
- Steyer JA, Horstmann H, and Almers W.** Transport, docking and exocytosis of single secretory granules in live chromaffin cells. *Nature* 388: 474–478, 1997.
- Suter DM and Forscher P.** An emerging link between cytoskeletal dynamics and cell adhesion molecules in growth cone guidance. *Curr Opin Neurobiol* 8: 106–116, 1998.
- Voets T, Neher E, and Moser T.** Mechanisms underlying phasic and sustained secretion in chromaffin cells from mouse adrenal slices. *Neuron* 23: 607–615, 1999.
- Wightman RM, Jankowski JA, Kennedy RT, Kawagoe KT, Schroeder TJ, Leszczyszyn DJ, Near JA, Diliberto EJ, and Viveros OH.** Temporally resolved catecholamine spikes correspond to single vesicle release from individual chromaffin cells. *Proc Natl Acad Sci USA* 88: 10754–10758, 1991.
- Xu T, Binz T, Niemann H, and Neher E.** Multiple kinetic components of exocytosis distinguished by neurotoxin sensitivity. *Nat Neurosci* 1: 192–200, 1998.
- Yang Y, Udayasankar S, Dunning J, Chen P, and Gillis KD.** A highly  $\text{Ca}^{2+}$ -sensitive pool of vesicles is regulated by protein kinase C in adrenal chromaffin cells. *Proc Natl Acad Sci USA* 99: 17060–17065, 2002.